A Macrocyclic Parallel Dimer Showing Quantum Coherence of Quintet Multiexcitons at Room Temperature

Wataru Ishii,[a†] Masaaki Fuki,[b,c†] Eman M Bu Ali,[d,j†] Shunsuke Sato,[e†] Bhavesh Parmar,[a] Akio Yamauchi,[a] Catherine Helenna Mulyadi,[a] Masanori Uji,[a] Samara Medina Rivero,[d,i] Go Watanabe,*[c,e,f,g] Jenny Clark,*[d] Yasuhiro Kobori,*[b,c,h] and Nobuhiro Yanai*[a,c]

[a]Department of Applied Chemistry, Graduate School of Engineering, Kyushu University, 744 Moto-oka, Nishi-ku, Fukuoka 819-0395, Japan.

[b]Molecular Photoscience Research Center, Kobe University, 1-1, Rokkodai-cho, Nada-ku, Kobe 657-8501, Japan.

[c]CREST, JST, Honcho 4-1-8, Kawaguchi, Saitama 332-0012, Japan.

[d]Department of Physics and Astronomy, The University of Sheffield, Sheffield S3 7RH, UK.

[e]Department of Physics, School of Science, Kitasato University, 1-15-1 Kitazato, Minami-ku, Sagamihara, Kanagawa, 252-0373, Japan.

[f]Department of Data Science, School of Frontier Engineering, Kitasato University, 1-15-1 Kitazato, Minami-ku, Sagamihara, Kanagawa, 252-0373, Japan.

[g]Kanagawa Institute of Industrial Science and Technology (KISTEC), 705–1 Shimoimaizumi, Ebina, Kanagawa 243–0435, Japan.

[h]Department of Chemistry, Graduate School of Science, Kobe University, 1-1, Rokkodai-cho, Nada-ku, Kobe 657-8501, Japan.

[i]Department of Physical Chemistry, Facultad de Ciencias, Universidad de Málaga, 29071 Málaga, Spain

[j]Department of Physics, College of Science, King Faisal University, Al-Hassa, Hofuf 31982, Saudi Arabia

[†]These authors contributed equally.

KEYWORDS: *Macrocyclic Parallel Dimer; Singlet Fission; Quintet Multiexciton; Quantum Coherence; Multilevel Qubits*

ABSTRACT: Singlet fission (SF) is a promising approach in quantum information science because it can generate spin-entangled quintet triplet pairs by photoexcitation independent of temperature. However, it is still challenging to rationally achieve quantum coherence at room temperature, which requires precise control of the orientation and dynamics of triplet pairs. Here we show that the quantum coherence of quintet multiexcitons can be achieved at room temperature by arranging two pentacene chromophores in parallel and close proximity within a macrocycle. By making dynamic covalent Schiff-base bonds between aldehyde-modified pentacene derivatives, macrocyclic parallel dimer-1 (**MPD-1**) can be selectively synthesized in a high yield. **MPD-1** exhibits fast sub-picosecond SF in polystyrene film and generates spin-polarized quintet multiexcitons. Furthermore, the coherence time T_2 of the **MPD-1** quintet is as long as 400 ns even at room temperature. This macrocyclic parallel dimer strategy opens up new possibilities for future quantum applications using molecular multilevel qubits.

INTRODUCTION

Quantum information science (QIS), an application of quantum mechanics, is revolutionizing a wide range of fields from computing to communications and sensing.[1-3] As the fundamental elements of QIS, molecular-based quantum bits (qubits) have the advantage that their structure is uniform at the atomic level and their structure and properties can be precisely controlled by chemical modification.[4-8] It is essential for any quantum applications to prepare the initial pure quantum state in the qubit and to have a sufficiently long quantum coherence time. As for initialization, cryogenic conditions are required to initialize qubits in thermal equilibrium, which severely limits the range of applications. On the other hand, molecular qubits composed of chromophores can generate non-equilibrium electron spin polarization, *i.e.*, the initialization state, by photoexcitation even under high temperature conditions such as room temperature.[7-9]

Among photo-initializable molecular qubits, singlet fission (SF) can generate a quintet triplet pair state with four entangled electrons, which should be useful for future two-qubit gate operation and highly sensitive quantum sensing.[10-20] Singlet excited state S_1, which is generated by photoexcitation, quickly becomes a singlet triplet pair state ^{1}TT, which is then converted to a quintet triplet pair state ^{5}TT by

spin evolution. Recent theoretical studies have shown that when the orientations of the chromophores are parallel, it is possible to selectively populate certain sub-levels of the quintet.[20, 21] Although many dimer compounds have been reported in which chromophores are covalently linked, in most cases the linkages contain single bonds and have structural freedom of rotation, which would suffer from decoherence.[22-26] While dimers linked by rigid linkers have been reported,[11, 13] quantum coherence of quintet multiexcitons at room temperature has not yet been observed.

Recently, quantum coherence of quintet multiexcitons has been observed for the first time at room temperature for pentacene chromophores densely arranged in a metal-organic framework (MOF), indicating that suppressed pentacene motion in the MOF structure is responsible for both the conversion from ^{1}TT to ^{5}TT and the quintet quantum coherence.[9] However, the quintet with long coherence time was a minor component due to the poor crystallinity of the MOF. It is desirable to construct a system that can produce quintet with long coherence time in a homogeneous structure. In particular, isolated dimer molecules in an inert host can function as multilevel qubits exhibiting long coherence times, since exciton diffusion-induced spin decoherence, as seen in MOFs and crystals,[12] is suppressed because of the absence of exciton diffusion. Furthermore, it is expected that the combination with microscopy techniques will enable quantum manipulations of electron spins in a single dimer molecule, which is promising for future applications in ultra-sensitive and ultra-high spatial resolution quantum sensing technologies.[27]

Here we report the synthesis of a macrocyclic parallel dimer (**MPD**) and the observation of quintet quantum coherence even at room temperature. A few macrocyclic compounds exhibiting SF have been synthesized, but in low yields or requiring special reaction systems.[28, 29] By employing the Schiff-base chemistry, which is commonly used for a dynamic covalent bond formation,[30-32] **MPD-1** with two pentacene chromophores can be selectively synthesized in a good yield (Figure 1a). The relatively rigid bridging structure including benzene ring together with the π-π interaction between pentacene units would suppress the rotational degree of freedom of the pentacene moieties and orient the pentacene units in parallel. This parallel proximity between adjacent pentacene would lead to ultrafast intramolecular SF and selective generation of the quintet states. **MPD-1** dispersed in polystyrene film exhibits the longest room-temperature coherence time T_2 of quintet of *ca.* 400 ns, indicating that the macrocyclic structure is a promising strategy for generating multilevel qubits that can be driven at room temperature.

RESULT AND DISCUSSION

The monomeric pentacene dialdehyde, 4,4'-(pentacene-6,13-diyl)dibenzaldehyde (**PDA**), was synthesized by following the previous report.[33] **MPD-1** was synthesized using **PDA** and *m*-xylylenediamine with a few drops of trifluoroacetic acid as a catalyst. The dynamic covalent bond chemistry such as Schiff-base formation can selectively produce the thermodynamically most stable compounds.[30, 34] In the current case, **MPD-1** was selectively obtained in a high isolated reaction yield of *ca.* 50%. The purity of **MPD-1** was fully confirmed by ^{1}H NMR spectroscopy (Figure S5), MALDI-TOF MS (Figure S6), high-resolution MS (Figure S7), and elemental analysis. Single-crystal X-ray diffraction (SCXRD) measurements of **MPD-1** revealed the parallel orientation between two pentacene units (Figure 1b and c). The proximate carbon-carbon distance between the two pentacene units is 3.3 to 3.7 Å, indicating the presence of π-π interactions. NMR measurements were performed to elucidate the dimer structure in CD_2Cl_2 solution at room temperature (Figure S4 and S5). The significant upfield shift of the pentacene protons in the dimer **MPD-1** in comparison with the monomer **PDA** indicates the π-π interactions between pentacene units are maintained in solution.

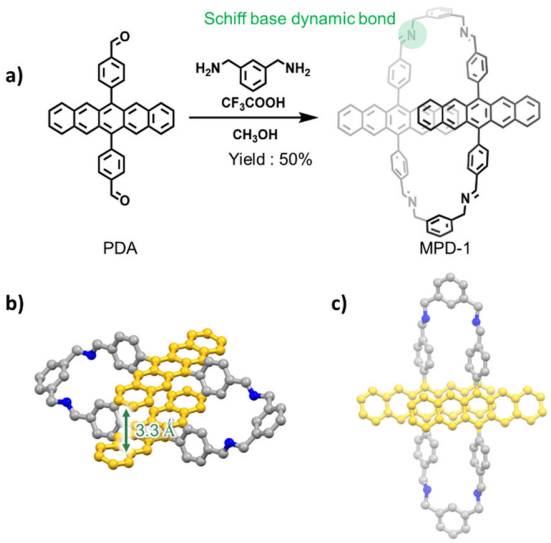

Figure 1. (a) Synthetic scheme of **MPD-1**. (b, c) Single crystal structure of **MPD-1**. (Solvent molecules and hydrogen atoms are omitted for clarity.)

Molecular dynamics (MD) simulations were performed to investigate whether the orientation between the pentacene units in **MPD-1** can be kept parallel when molecularly dispersed (Figure 2a and 2b). A single molecule of **MPD-1** was placed in the center of the cubic MD cell and the remaining space was filled with toluene molecules, which were used as the initial structure for MD simulations. In the system at 300 K, **MPD-1** was found to maintain the distance between the centers of the mass of the pentacene units around 5.5 Å for most of the time (Figure 2c), which is close to the center-to-center distance in the XRD structure of 5.5 Å. Two types of angles between the long axis vectors of the pentacene in the plane perpendicular (θ) and parallel (φ) to the aromatic ring planes did not take the significant values; the average values during the last 400 ns were θ = 9±9 degree and φ = 8±8 degrees, respectively (Figure 2d and 2e). It indicates that the pentacene units remained parallel for most of the time while they were occasionally tilted and moved back and forth and from side to side due to thermal fluctuations, as recently demonstrated in the exciton pairs in linked parallel pentacene dimers. In toluene glass at a lower temperature of 80 K, the fluctuations of the distance between the centers of the mass of the adjacent pentacene were smaller and the structure in solution was maintained (Figure S8).

The excitonic interactions between pentacene chromophores in the dimer structure were investigated from the absorption spectra of **MPD-1** at room temperature. Beer-Lambert plots of toluene solutions of **MPD-1** showed that it is in the molecularly dispersed state up to 200 μM (Figure S9). Absorption spectra of **PDA** and **MPD-1** in toluene at room temperature showed a slight broadening of the spectrum with a redshift of the peak from 601.5 nm to 611.5 nm for the dimer compared to the monomer (Figure S10). This is due to excitonic interactions between neighboring pentacene chromophores, which is consistent with the dimer structure with pentacene moieties in close proximity observed in NMR measurements and MD simulations.

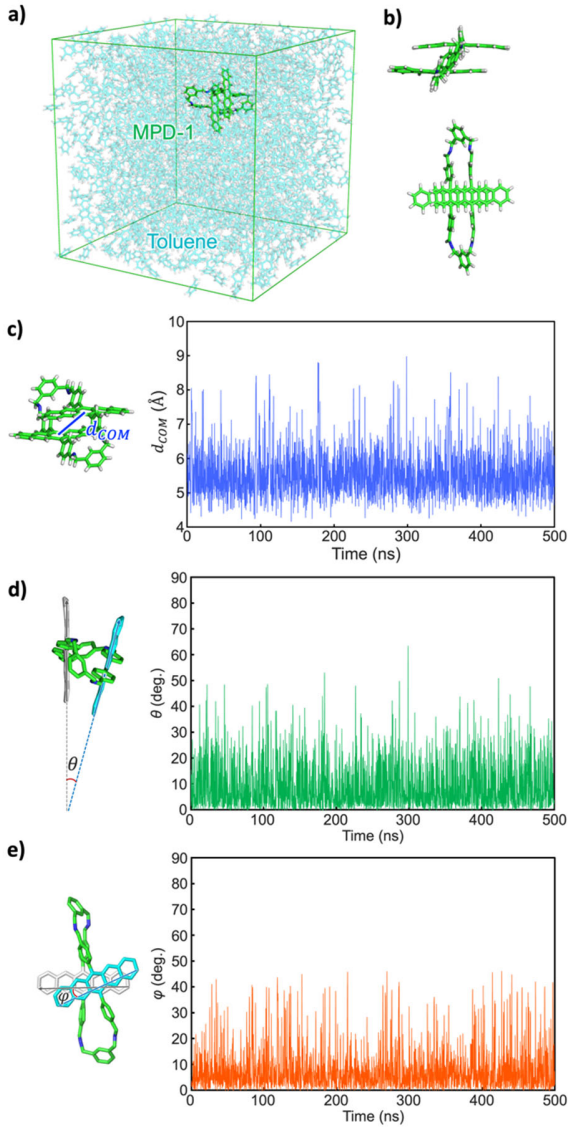

Figure 2. Snapshots of MD simulation at 300 K in equilibrium for (a) the whole system and (b) only **MPD-1**. Time dependences during the 500 ns of (c) the distance between the centers of the mass of the pentacene units of **MPD-1** and two types of angles between the long axis vectors of the pentacene units in the plane (d) perpendicular and (e) parallel to the aromatic ring planes, θ and φ, respectively.

The emission spectra of the monomer and dimer samples are strikingly similar when taking self-absorption into account (Figure S10). This spectral similarity, together with observations from the transient spectroscopy described below, suggests that the 45-fold weaker photoluminescence from the dimer sample is from a minority of emissive monomer 'impurities' in the sample. As we discuss below, these may originate from photo-damaged or dissociated dimers and indicate a need to improve the stability of the dimer in the future work. Nevertheless, the dominant photophysics we study in this work originates from the dimers, with monomers contributing a very minor component, as indicated by the absorption and transient absorption spectroscopy described below.

Since it is necessary to evaluate the spin properties in the solid state by EPR measurement, we also measured optical properties of **MPD-1** dispersed in polystyrene film. The absorption spectrum of **MPD-1** in polystyrene indicates its molecular dispersion with no change in peak position and shape up to 5 mol% (Figure S12). The absorption spectrum of **MPD-1** in polystyrene is close to that in toluene solution, indicating that the same dimer structure is maintained in polystyrene (Figure S13).

Transient absorption spectroscopy (TAS) measures the signature of excited states as a function of time after excitation, allowing us to track their evolution from femtoseconds to milliseconds. In Figure 3, we show TAS of **PDA** monomer and **MPD-1** dimer measured in polystyrene films at 0.05 mol% with excitation at 532 nm. We chose these conditions for ease of comparison with EPR measurements in Figure 4 and 5, but find that at these concentrations, the TAS behavior does not depend on concentration (Figure S20) between 0.05 mol% and 0.005 mol% (at the limit of our ability to measure TAS), suggesting that the majority of the doped molecules are well isolated from each other and show no signs of inter-dimer aggregation at 0.05 mol%.

Selected TAS spectra and dynamics of the **PDA** monomer, are shown in Figure 3a and 3b (the full TAS spectra/dynamics are shown in figure S14 to S16). Our results reproduce the reported behavior of pentacene monomers in solution: at early times, represented by the 10 ps spectrum (blue) in Figure 3a, the spectra are dominated by singlet S_1 states exhibiting a strong excited state absorption (ESA) band peaked at *ca.* 450 nm (452 nm for **PDA**). Over nanosecond timescales, the spectrum evolves, due to intersystem crossing (ISC) to form triplets.[35] The triplets are characterized by vibronically structured ESA bands with a dominant peak at *ca.* 530 nm (514 nm for **PDA**), represented by the brown spectrum taken at 200 ns pump-probe delay in Figure 3. The ISC-generated triplets in this sample decay with a ~50 μs time-constant (Figure S14).

Conversely, selected TAS spectra/dynamics of **MPD-1** dimer in Figure 3c and 3d (full spectra/dynamics in Figure S17 to S20) show the formation of only one excited species on the measured timescales. This species decays with only minor spectral evolution from 100 fs (light green) to beyond 1 μs (dark green). Given the similarity of this spectrum to the monomer triplet spectrum in Figure 3a (reproduced in brown in Figure 3b for ease of comparison), we assign the **MPD-1** TAS spectrum to triplets. The rapid sub-100 fs

generation of these triplets in **MPD-1** suggests that they are generated by SF within our instrument response time (≤100 fs). In the dimer, the triplet signatures initially decay rapidly (10s of nanoseconds), orders of magnitude faster than the ISC-generated triplets on isolated molecules (compare figure 3b and 3d), as expected for SF-generated triplets. This rapid decay is associated with the spin-allowed non-radiative decay of the strongly exchange-coupled ^{1}TT triplet pair state, the initial triplet pair state of SF.[36]

Following the initial decay, the remaining population decays on a slower timescale. Initially, the spectra are similar to those at the earliest times; compare the spectra at 200 ns and 100 fs in Figure 3c, for example. We assign the triplet signatures on these 10-100s of nanosecond timescales to triplet pairs with quintet character, ^{5}TT, formed from ^{1}TT via spin evolution, rather than to isolated triplets. We make this assignment for three reasons: (1) the slower decay implies spin-forbidden decay to the singlet ground state, and therefore it is unlikely to be due to ^{1}TT population; (2) the ESA spectrum on these timescales (200 ns) is the same as the early-time ^{1}TT spectrum (100 fs), but different to the monomer ESA triplet spectrum (brown) and therefore is likely to be a triplet pair state on the dimer, rather than isolated triplets; (3) for symmetry reasons, it is most likely that ^{1}TT converts to ^{5}TT rather than ^{3}(TT).[37] This assignment is confirmed by TREPR measurements described below.

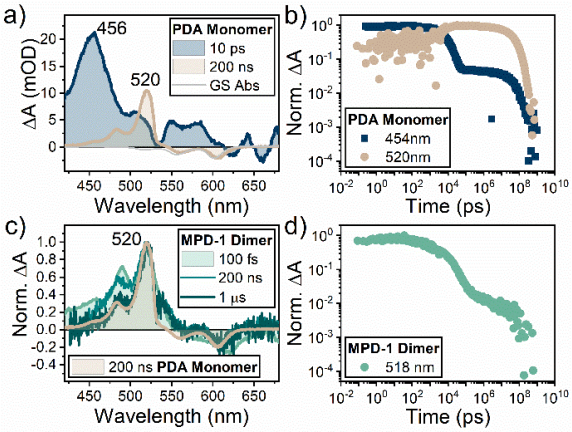

Figure 3. Selected TAS spectra (a, c) and their corresponding kinetics in the full-time window (from ps to ms) (b, d) of (a, b) **PDA** monomer in polystyrene film (0.05 mol%) at room temperature; and (c, d) **MPD-1** dimer in polystyrene film (0.05 mol%) at room temperature. In the monomer (a, b), singlet states (blue) evolve to form triplets by intersystem crossing (brown). In the dimer (c, d), triplet signatures are present from 100 fs (green). Ground state absorption spectra are also shown for reference (grey shadowed lines).

Before describing the EPR results, we note that the TAS spectral shape in **MPD-1** evolves to form the 1 μs spectrum reported in figure 3c that is identical to the ISC-generated triplets on the **PDA** monomer (the differences around 532 nm are artifacts from different pump scatter in the different experiments). These states could be due to ISC-generated triplets on monomer impurities in the dimer sample or could indicate uncoupled triplet pairs on dimers. Given the emission spectral features assigned to monomer emission described above and results from the EPR reported below, we conclude that these ≥ 1 μs features are from ISC-generated triplets on monomer impurities in the sample. The TAS signature from these monomers is weak, for example we see negligible evidence of early-time singlet ESA at 456 nm, and therefore conclude that the proportion of monomers within the dimer sample is small, a conclusion supported by the absorption/emission spectroscopy described above.

We also observe that the strongly exchange coupled triplet pair in the dimer, ^{1}TT at ~100 fs shows no shift of the main ESA band compared with the monomer triplet ESA; a shift has previously been associated with the triplet pair binding energy.[38] This could suggest that the exchange coupling in this dimer is smaller than in previously measured systems.[36]

Finally, we note that TAS of **MPD-1** in toluene shows identical ESA ^{1}TT signatures at early times similar to **MPD-1** dispersed in polystyrene films (Figure S19), confirming SF in the isolated dimers. However, in solution, where the dimer is unhindered by the polymer matrix, ^{1}TT decays to the ground state with a ~60 ps time constant, much faster than in the polymer film. We speculate that this short lifetime is due to efficient non-radiative decay, enabled by conformational reorganization in the solution environment. In solution, at room temperature, therefore, ^{1}TT does not live long enough to form quintets.

Continuous-wave transient electron paramagnetic resonance (CW-TREPR) measurement of **MPD-1** in polystyrene film was conducted at room temperature (Figure 4a and 4b). The highly symmetric spin polarization signals with A/A/E/A/E/E pattern were observed, which is the typical signal of SF-derived quintets. In addition, no triplet signal in outer side than quintet was observed. This implies the dissociated triplets from triplet pairs were not generated due to the strong π-π interaction by the rigid bridge between the close-contact pentacene units in the macrocyclic structure (Figure 4c). After prolonged laser irradiation, the sample showed a color change (Figure S30). No signal was observed in the steady-state CW-EPR spectrum before the laser irradiation, while some signals were detected after the TREPR and pulsed EPR measurements (Figure S29). These results suggest a partial photo-induced decomposition of **MPD-1** in polystyrene. As noted above, improving the photostability of the dimer is an important future task.

The TA spectroscopy described above suggests that after excitation with 532 nm laser, the initially generated ^{1}TT can be converted to quintet triplet pair (^{5}TT). Our calculations suggest this occurs by the modulation of spin-spin exchange interaction J (Figure 4c). In this case, the J modulation would be induced by the chromophore fluctuation.[21] Based on this theory, we performed the simulation of TREPR spectrum with two quintet exciton conformations ($^5TT_1$ and $^5TT_2$) using the density matrix formalism analysis.

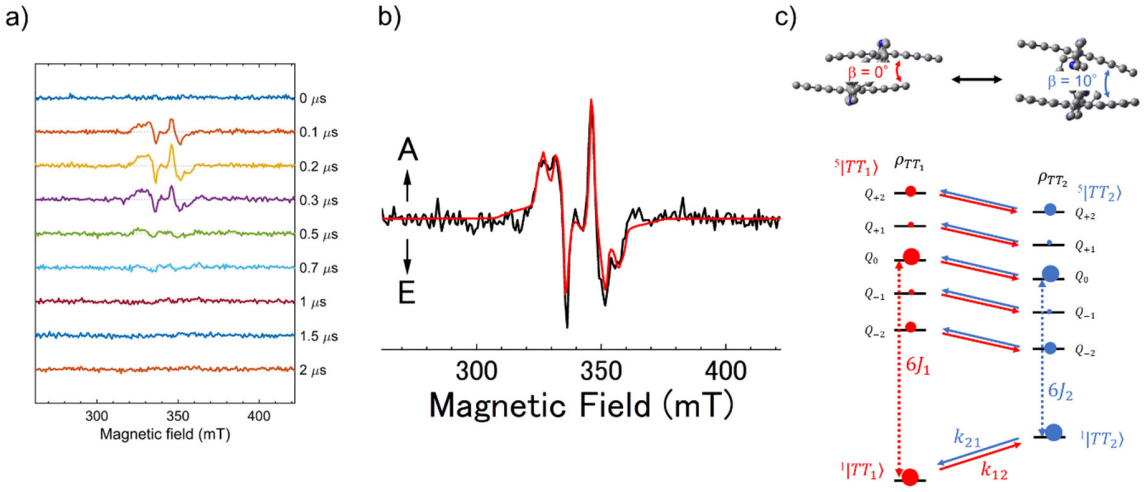

Figure 4. (a) Time evolution of TREPR spectra of **MPD-1** in polystyrene at room temperature. (b) Spectrum simulation of TREPR at 200 ns after laser irradiation using the density matrix formalism analysis. (c) Schematic image of quintet polarization generation through the fluctuation of exchange interaction.

The EPR spectrum was simulated by assuming **MPD-1** dimers with two different conformations of the dihedral angle between the aromatic planes, 0° and 10°, as the stable $^5TT_1$ and the activated $^5TT_2$ by an energy of 80 cm^{-1}, respectively. We also assumed that the structural fluctuations between them modulate the exchange coupling J to generate quintet triplet pairs (Figure 4c). This is in good agreement with the dimer fluctuations observed in the MD simulation for toluene solution, suggesting that the angle of molecular fluctuations in polystyrene film is similar to those in toluene solution.

The negative exchange coupling J represents that ^5TT is more energetically unstable than ^1TT and is responsible for the fast deactivation of the quintets. Transient absorption measurements show that the ^1TT lifetime in toluene solution is very short (60 ps), whereas in polystyrene it is relatively long (10-100 ns). This suggests that the large structural fluctuations of **MPD-1,** as seen in the MD simulations of toluene solution, should be suppressed in the rigid polystyrene matrix. However, small fluctuations of **MPD-1** (10-degree angle change) may result in the quintet generation because J would substantially be modulated by the subtle angle changes (Figure 4c).

When the principal axes of the pentacene units in the dimer are aligned to parallel, sublevel-selective transition from ^1TT to ^5TT occurs based on the anisotropic terms in the spin Hamiltonian. In the polystyrene matrix, the parallel orientation of **MPD-1** was maintained, resulting in the highly symmetric EPR spectrum (Figure 4b). This spectrum shape represents the selective population distribution of quintet sublevels of Q_0 and $Q_{\pm2}$ thanks to the parallel orientation of **MPD-1**. The selectivity would be further enhanced when the dimers take a certain orientation to the external magnetic field.

By simulating the case that **MPD-1** is aligned parallelly against the external magnetic field ($B_0||z$), the maximized selective population distribution of quintets was observed (Figure S23). This result is in good agreement with the previous theoretical studies,[20, 21] indicating that **MPD-1** can work as a high-quality multilevel qubit that produces pure quintet states.

Note that when the TREPR was measured again one month after the first measurement, additional triplet signal originating from ISC was also observed. This suggests that even under vacuum conditions, **MPD-1** can be slowly photo-decomposed to partially produce monomers (Figure S24).

In order to assign the spin multiplicities of EPR signals, we performed a nutation measurement of **MPD-1** using X-band pulsed EPR (Figure 5b). The nutation signals were obtained under the magnetic fields fixed at the peak tops of the echo-detected EPR spectrum (Figure 5a) and Fourier transformed (Figure 5b). Nutation frequencies of a transition ($\Delta m_S = \pm1$) are represented as a following equation;

$$\omega = \frac{g\mu_B B_1}{\hbar}\sqrt{S(S+1) - m_S(m_S \pm 1)}$$

where g is the g-value, μ_B is the Bohr magneton, $\hbar$ is the reduced Planck constant and B_1 is the effective magnetic field strength of the microwave pulse. Therefore, nutation frequency ratio is represented as doublet: triplet: quintet ($Q_{\pm1} \leftrightarrow Q_{\pm2}$): quintet ($Q_0 \leftrightarrow Q_{\pm1}$) = 1: $\sqrt{2}$: 2: $\sqrt{6}$. In the spin nutation measurements, the nutation frequency ratio of 1.00: 1.46: 2.16: 2.68 was obtained, which approximately coincides with the theoretical values. Furthermore, we measured the delay time (t_{delay}) dependence between the microwave pulses and the laser flash on the echo signal (Figure 5c). The quick rise in the quintet echo originates from deactivation rate constant in the singlet TT with k_{Rec} = 2.0×10^7 s^{-1} (Table S3). This is due to the quick deactivation

of ^{1}TT, the source of quintet generation. This singlet TT deactivation kinetics is in good agreement with the initial rapid decay (10s of nanoseconds) observed in the TA signal.

The ^{1}TT –> ^{5}TT$_0$ spin relaxation time constant is thus obtained to be 534 ns from the echo signal decay in Figure 5c. This is close to the decay time constant (283 ns) of the quintet signal obtained by CW-TREPR at reduced microwave power (Figure S27).

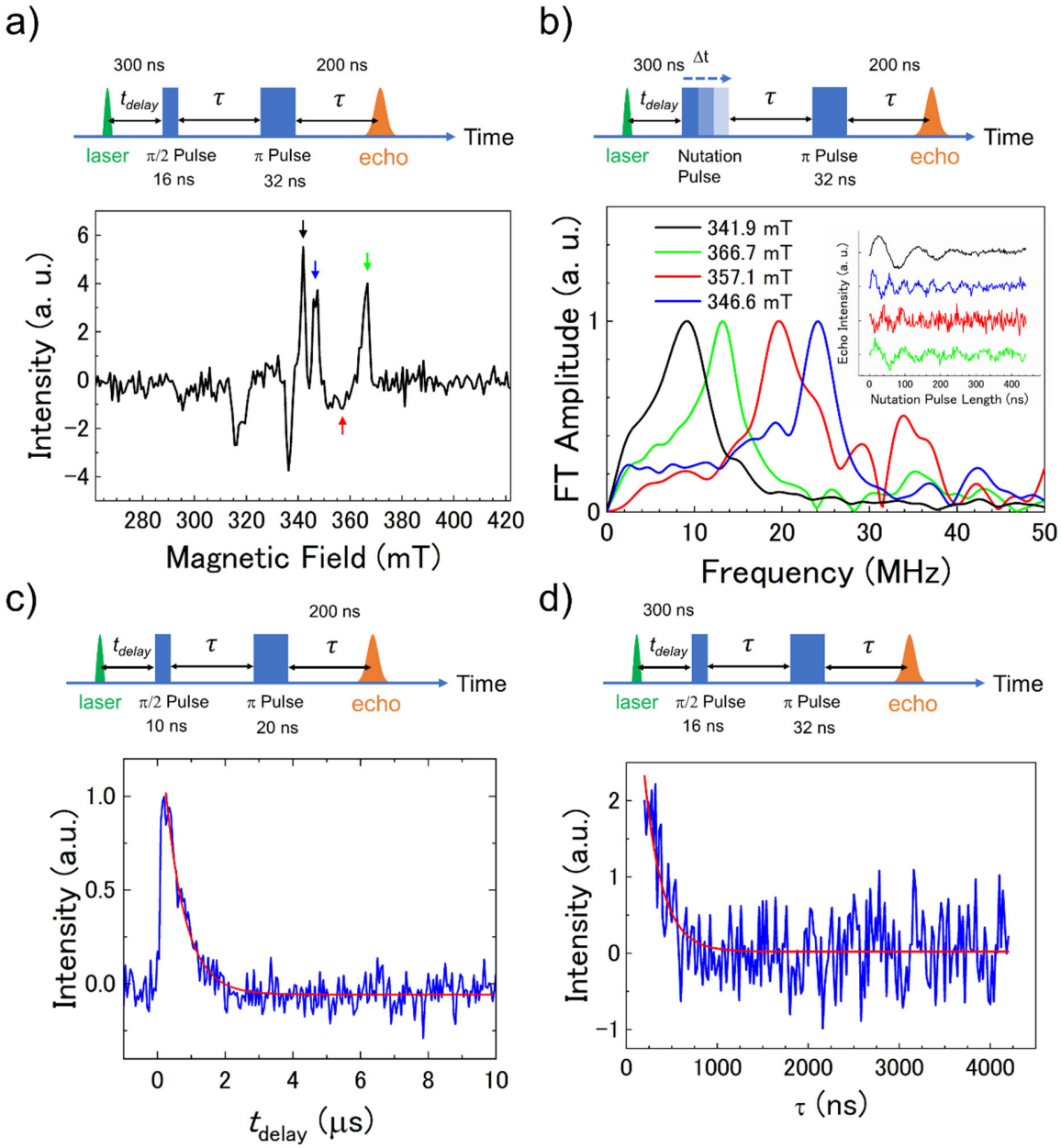

Figure 5. (a) An echo detected spectrum (bottom) of **MPD-1** in polystyrene obtained by 532 nm laser irradiations at room temperature and its pulse sequence (top). The pulse sequence was employed as laser–t_{delay}–t_1–τ_{echo}–t_2– τ_{echo}–echo. The durations of the first pulse (t_1) and the second pulse (t_2) are 16 ns and 32 ns, respectively. The delay time of t_{delay} and τ_{echo} are 300 ns and 200 ns, respectively. Spin nutation measurements were carried out at the magnetic field indicated by arrows. (b) Fourier transformed spin nutation signals. Inset shows time profiles of spin nutation signals with baseline corrections. The peaks of the nutation frequencies at the magnetic field, indicated by the arrows in Fig. 5a, were 9.03, 13.18, 19.53, and 24.17 MHz, respectively. (c) Dependence of t_{delay} of the echo intensity at 346.6 mT (blue line) employing π/2 = 10 ns, π = 20 ns and τ_{echo} = 200 ns with a fitting line (red line). The ^{5}TT$_0$ spin relaxation time obtained from the echo signal decay was 534 ns. (d) Coherence time (T_2) of the quintet triplet pairs. A pulse sequence of the Hahn echo detection (laser- t_{delay} - t_1-τ_{echo}-t_2-τ_{echo}-echo) used in the measurement with t_1 = 16 ns, t_2 = 32 ns and τ_{echo} = 200 ns. T_2 = 395 ns was obtained by plotting the echo signal with varying τ_{echo} at B$_0$ = 346.6 mT with t_{delay} = 300 ns.

This means that the components observed in the spin echoes are the major components in the system, *i.e.*, the dimers are well dispersed in the polystyrene matrix and in a uniform environment. The slight difference in the two time constants is probably due to the fact that the decay time of CW-TREPR is influenced by the high power intensity of the irradiated continuous microwave in the dielectric resonator.[12] While previously report on Pn-MOF concluded that the quintets observed in CW-TREPR and pulsed EPR comes from different components due to low crystallinity,[9] in this study, the dimers are uniformly dispersed in polystyrene and the signals observed in CW-TREPR and pulsed EPR should be derived from the same component. In addition, overlapping the kinetics of TA signal at 488 nm and the kinetics of the echo signal obtained by pulsed EPR shows relatively good agreement on the 100-1000s of nanosecond timescales, indicating good consistency between TA and EPR regarding the quintet dynamics (Figure S29).

In addition to the triplet signal, a signal derived from radical was also observed in the subsequent pulsed EPR, suggesting degradation of pentacene itself: the sample after TREPR and pulsed EPR measurements was discolored only in the light-irradiated area, confirming the degradation of pentacene (Figure S30).

In the spin coherence time (T_2) measurements of **MPD-1** by the Hahn echo detection (Figure 5d), notably long T_2 of 395 ns was observed even at room temperature. The quintet is generated by J modulation with slight conformation change (Figure 4c), and the large and random fluctuation of anisotropic zero-field splitting interactions should not dominate in this system. This relatively long coherence time opens the possibility of quintet spins as multilevel qubits that can be driven even at room temperature.[9] The T_2 obtained in the present study is about three times longer than that in the MOF (120 - 150 ns). The reason for longer T_2 may be due to the absence of phonon effect by the molecular aggregation in the present dispersed dimer system, reflecting the suppressive fluctuations of the solid polystyrene environment at room temperature. This is very different from the kinetic behavior in toluene shown in Figure 2, and an ideal environment for generating spin quantum nature. As pointed out previously, there is a trade-off between quintet generation efficiency and spin coherence time.[11] The quintet generation efficiency in **MPD-1** dimer was low (<1 %). This is consistent with long coherence time due to the lack of decoherence through mixing of ^{1}TT and ^{5}TT. On the contrary, when the quintet generation efficiency is high, the fast spin evolution from ^{5}TT to ^{1}TT leads to a shorter quintet spin coherence time.

CONCLUSION

In conclusion, we have shown that the macrocyclic parallel dimer is an appropriate molecular design for exhibiting a long coherence time T_2 of quintet state even at room temperature. The use of dynamic covalent Schiff base chemistry allowed us to easily synthesize the **MPD-1** dimer in high yield, and the macrocyclic structure keeps the pentacene units oriented parallel to each other in close proximity in solution or polymer matrix, leading to ultrafast SF of less than 100 fs and allowing the selective population of specific quintet sublevels. The structural fluctuations of the pentacene units in the **MPD-1** dimer were kept small, and the longest room-temperature quintet coherence time to date of nearly 400 ns was achieved. Unlike previous MOF systems, the homogeneously dispersed dimers have the advantage that the component with the long coherence time is major. Further fine tuning of linker and chromophore structures would provide a wide range of attractive MPDs from a viewpoint of flexibility, distance, orientation, and stability. In addition to the potential of strict structural control, optically-detected magnetic resonance at the single-molecule level will be possible by using chromophores that exhibit delayed fluorescence due to triplet-triplet annihilation, the reverse process of SF. The multilevel qubits, whose structure can be strictly defined at the atomic level, and which have long coherence time, would be very powerful in elucidating a wide range of biological and physical phenomena in the future.

AUTHOR INFORMATION

Corresponding Author

*go0325@kitasato-u.ac.jp (G.W.); jenny.clark@sheffield.ac.uk (J.C.); ykobori@kitty.kobe-u.ac.jp (Y.K.); yanai@mail.cstm.kyushu-u.ac.jp (N.Y.)

Author Contributions

N.Y. designed the project. W.I. carried out the synthesis and characterizations of the dimer with the contribution of A.Y., B.P, C.H.M., and M.U. S.S. and G.W. conducted the MD simulation. E.M.B.A., S.M.R., J.C., and W.I. carried out the TA measurements and analysis. M.F., Y.K., and W.I. conducted the EPR measurements and analysis. W.I., M.F., E.M.B.A., S.S., A.Y., B.P., S.M.R., G.W., J.C., Y.K., and N.Y. wrote the paper with contributions from all the authors.

Notes

The authors declare no competing financial interests.

ACKNOWLEDGMENT

This work was partly supported by the JST-CREST Program (JPMJCR23I6 and JPMJCR23O1), JSPS KAKENHI (JP23H00304, JP23KJ1717, JP22K19051, JP20H05832, JP20K21174, JP22H00344, JP23H00309, JP20KK0120, JP22K19008, JP23KJ1694), Kyushu University Platform of Inter-/Transdisciplinary Energy Research (Q-PIT) through its "Module-Research Program", and the Kyushu University Integrated Initiative for Designing Future Society. This work was partially carried out by the joint research program of Molecular Photoscience Research Center, Kobe University. The computations were partially performed at the Research Center for Computational Science, Okazaki, Japan (Project: 23-IMS-C038). S. M. R. thanks the Spanish Ministry of Universities and the University of Málaga for her Margarita Salas postdoctoral fellowship under the "Plan de Recuperación, Transformación y Resiliencia" funded by European Union-Next Generation EU. E.M.B. thanks King Faisal University, Al-Hassa, Saudi Arabia for her PhD scholarship, and acknowledges support from Saudi Arabian Cultural Bureau in London. E. M. B. A., S. M. R. and J. C. also thank EPSRC

for enabling this research through grants EP/T012455, EP/L022613 and EP/R042802. Y. K. thanks Professor C. W. M. Kay (Saarland University) for his kind modification of the dielectric resonator for sensitive pulsed EPR measurements in Kobe University.

REFERENCES

(1) Divincenzo, D. P. The Physical Implementation of Quantum Computation. *Fortschr. Phys.* **2000**, *48* (9-11), 771-783.

(2) Bhaskar, M. K.; Riedinger, R.; Machielse, B.; Levonian, D. S.; Nguyen, C. T.; Knall, E. N.; Park, H.; Englund, D.; Lončar, M.; Sukachev, D. D.; et al. Experimental demonstration of memory-enhanced quantum communication. *Nature* **2020**, *580* (7801), 60-64.

(3) Degen, C. L.; Reinhard, F.; Cappellaro, P. Quantum sensing. *Rev. Mod. Phys.* **2017**, *89* (3).

(4) Wasielewski, M. R.; Forbes, M. D. E.; Frank, N. L.; Kowalski, K.; Scholes, G. D.; Yuen-Zhou, J.; Baldo, M. A.; Freedman, D. E.; Goldsmith, R. H.; Goodson, T., 3rd; et al. Exploiting chemistry and molecular systems for quantum information science. *Nat. Rev. Chem.* **2020**, *4* (9), 490-504.

(5) Bayliss, S. L.; Laorenza, D. W.; Mintun, P. J.; Kovos, B. D.; Freedman, D. E.; Awschalom, D. D. Optically addressable molecular spins for quantum information processing. *Science* **2020**, *370* (6522), 1309-1312.

(6) Stein, B. W.; Tichnell, C. R.; Chen, J.; Shultz, D. A.; Kirk, M. L. Excited State Magnetic Exchange Interactions Enable Large Spin Polarization Effects. *J. Am. Chem. Soc.* **2018**, *140* (6), 2221-2228.

(7) Maylander, M.; Thielert, P.; Quintes, T.; Vargas Jentzsch, A.; Richert, S. Room Temperature Electron Spin Coherence in Photogenerated Molecular Spin Qubit Candidates. *J. Am. Chem. Soc.* **2023**, *145* (25), 14064-14069.

(8) Gorgon, S.; Lv, K.; Grune, J.; Drummond, B. H.; Myers, W. K.; Londi, G.; Ricci, G.; Valverde, D.; Tonnele, C.; Murto, P.; et al. Reversible spin-optical interface in luminescent organic radicals. *Nature* **2023**, *620* (7974), 538-544.

(9) Yamauchi, A.; Tanaka, K.; Fuki, M.; Fujiwara, S.; Kimizuka, N.; Ryu, T.; Saigo, M.; Onda, K.; Kusumoto, R.; Ueno, N.; et al. Room-temperature quantum coherence of entangled multiexcitons in a metal-organic framework. *Sci. Adv.* **2024**, *10* (1).

(10) Collins, M. I.; McCamey, D. R.; Tayebjee, M. J. Y. Fluctuating exchange interactions enable quintet multiexciton formation in singlet fission. *J. Chem. Phys.* **2019**, *151* (16), 164104.

(11) Dill, R. D.; Smyser, K. E.; Rugg, B. K.; Damrauer, N. H.; Eaves, J. D. Entangled spin-polarized excitons from singlet fission in a rigid dimer. *Nat. Commun.* **2023**, *14* (1).

(12) Jacobberger, R. M.; Qiu, Y.; Williams, M. L.; Krzyaniak, M. D.; Wasielewski, M. R. Using Molecular Design to Enhance the Coherence Time of Quintet Multiexcitons Generated by Singlet Fission in Single Crystals. *J. Am. Chem. Soc.* **2022**, *144* (5), 2276-2283.

(13) Lin, L.-C.; Smith, T.; Ai, Q.; Rugg, B. K.; Risko, C.; Anthony, J. E.; Damrauer, N. H.; Johnson, J. C. Multiexciton quintet state populations in a rigid pyrene-bridged parallel tetracene dimer. *Chem. Sci.* **2023**, *14* (41), 11554-11565.

(14) Lubert-Perquel, D.; Salvadori, E.; Dyson, M.; Stavrinou, P. N.; Montis, R.; Nagashima, H.; Kobori, Y.; Heutz, S.; Kay, C. W. M. Identifying triplet pathways in dilute pentacene films. *Nat. Commun.* **2018**, *9* (1).

(15) MacDonald, T. S. C.; Tayebjee, M. J. Y.; Collins, M. I.; Kumarasamy, E.; Sanders, S. N.; Sfeir, M. Y.; Campos, L. M.; McCamey, D. R. Anisotropic Multiexciton Quintet and Triplet Dynamics in Singlet Fission via Pulsed Electron Spin Resonance. *J. Am. Chem. Soc.* **2023**, *145* (28), 15275-15283.

(16) Matsuda, S.; Oyama, S.; Kobori, Y. Electron spin polarization generated by transport of singlet and quintet multiexcitons to spin-correlated triplet pairs during singlet fissions. *Chem. Sci.* **2020**, *11* (11), 2934-2942.

(17) Orsborne, S. R. E.; Gorman, J.; Weiss, L. R.; Sridhar, A.; Panjwani, N. A.; Divitini, G.; Budden, P.; Palecek, D.; Ryan, S. T. J.; Rao, A.; et al. Photogeneration of Spin Quintet Triplet-Triplet Excitations in DNA-Assembled Pentacene Stacks. *J. Am. Chem. Soc.* **2023**, *145* (9), 5431-5438.

(18) Bayliss, S. L.; Weiss, L. R.; Kraffert, F.; Granger, D. B.; Anthony, J. E.; Behrends, J.; Bittl, R. Probing the Wave Function and Dynamics of the Quintet Multiexciton State with Coherent Control in a Singlet Fission Material. *Phys. Rev. X* **2020**, *10* (2).

(19) Rugg, B. K.; Smyser, K. E.; Fluegel, B.; Chang, C. H.; Thorley, K. J.; Parkin, S.; Anthony, J. E.; Eaves, J. D.; Johnson, J. C. Triplet-pair spin signatures from macroscopically aligned heteroacenes in an oriented single crystal. *Proc. Natl. Acad. Sci.* **2022**, *119* (29).

(20) Smyser, K. E.; Eaves, J. D. Singlet fission for quantum information and quantum computing: the parallel JDE model. *Sci. Rep.* **2020**, *10* (1).

(21) Kobori, Y.; Fuki, M.; Nakamura, S.; Hasobe, T. Geometries and Terahertz Motions Driving Quintet Multiexcitons and Ultimate Triplet–Triplet Dissociations via the Intramolecular Singlet Fissions. *J. Phys. Chem. B* **2020**, *124* (42), 9411-9419.

(22) Sanders, S. N.; Kumarasamy, E.; Pun, A. B.; Trinh, M. T.; Choi, B.; Xia, J.; Taffet, E. J.; Low, J. Z.; Miller, J. R.; Roy, X.; et al. Quantitative Intramolecular Singlet Fission in Bipentacenes. *J. Am. Chem. Soc.* **2015**, *137* (28), 8965-8972.

(23) Zirzlmeier, J.; Lehnherr, D.; Coto, P. B.; Chernick, E. T.; Casillas, R.; Basel, B. S.; Thoss, M.; Tykwinski, R. R.; Guldi, D. M. Singlet fission in pentacene dimers. *Proc. Natl. Acad. Sci.* **2015**, *112* (17), 5325-5330.

(24) Sakai, H.; Inaya, R.; Nagashima, H.; Nakamura, S.; Kobori, Y.; Tkachenko, N. V.; Hasobe, T. Multiexciton Dynamics Depending on Intramolecular Orientations in Pentacene Dimers: Recombination and Dissociation of Correlated Triplet Pairs. *J. Phys. Chem. Lett.* **2018**, *9* (12), 3354-3360.

(25) Lukman, S.; Musser, A. J.; Chen, K.; Athanasopoulos, S.; Yong, C. K.; Zeng, Z.; Ye, Q.; Chi, C.; Hodgkiss, J. M.; Wu, J.; et al. Tuneable Singlet Exciton Fission and Triplet–Triplet Annihilation in an Orthogonal Pentacene Dimer. *Adv. Funct. Mater.* **2015**, *25* (34), 5452-5461.

(26) Majumder, K.; Mukherjee, S.; Panjwani, N. A.; Lee, J.; Bittl, R.; Kim, W.; Patil, S.; Musser, A. J. Controlling Intramolecular Singlet Fission Dynamics via Torsional Modulation of Through-Bond versus Through-Space Couplings. *J. Am. Chem. Soc.* **2023**, *145* (38), 20883-20896.

(27) Reid, O. G.; Johnson, J. C.; Eaves, J. D.; Damrauer, N. H.; Anthony, J. E. Molecular Control of Triplet-Pair Spin Polarization and Its Optoelectronic Magnetic Resonance Probes. *Acc. Chem. Res.* **2024**, *57* (1), 59-69.

(28) Kuroda, K.; Yazaki, K.; Tanaka, Y.; Akita, M.; Sakai, H.; Hasobe, T.; Tkachenko, N. V.; Yoshizawa, M. A Pentacene‐based Nanotube Displaying Enriched Electrochemical and Photochemical Activities. *Angew. Chem. Int. Ed.* **2019**, *58* (4), 1115-1119.

(29) Bergman, H. M.; Kiel, G. R.; Witzke, R. J.; Nenon, D. P.; Schwartzberg, A. M.; Liu, Y.; Tilley, T. D. Shape-Selective Synthesis of Pentacene Macrocycles and the Effect of Geometry on Singlet Fission. *J. Am. Chem. Soc.* **2020**, *142* (47), 19850-19855.

(30) Rowan, S. J.; Cantrill, S. J.; Cousins, G. R. L.; Sanders, J. K. M.; Stoddart, J. F. Dynamic Covalent Chemistry. *Angew. Chem. Int. Ed.* **2002**, *41* (6), 898-952.

(31) Hasell, T.; Wu, X.; Jones, J. T. A.; Bacsa, J.; Steiner, A.; Mitra, T.; Trewin, A.; Adams, D. J.; Cooper, A. I. Triply interlocked covalent organic cages. *Nat. Chem.* **2010**, *2* (9), 750-755.

(32) Tozawa, T.; Jones, J. T. A.; Swamy, S. I.; Jiang, S.; Adams, D. J.; Shakespeare, S.; Clowes, R.; Bradshaw, D.; Hasell, T.; Chong, S. Y.; et al. Porous organic cages. *Nat. Mater.* **2009**, *8* (12), 973-978.

(33) Fujiwara, S.; Hosoyamada, M.; Tateishi, K.; Uesaka, T.; Ideta, K.; Kimizuka, N.; Yanai, N. Dynamic Nuclear Polarization of Metal-Organic Frameworks Using Photoexcited Triplet Electrons. *J. Am. Chem. Soc.* **2018**, *140* (46), 15606-15610.

(34) Jin, Y.; Yu, C.; Denman, R. J.; Zhang, W. Recent advances in dynamic covalent chemistry. *Chem. Soc. Rev.* **2013**, *42* (16), 6634-6654.

(35) Papadopoulos, I.; Zirzlmeier, J.; Hetzer, C.; Bae, Y. J.; Krzyaniak, M. D.; Wasielewski, M. R.; Clark, T.; Tykwinski, R. R.; Guldi, D. M. Varying the Interpentacene Electronic Coupling to Tune Singlet Fission. *J. Am. Chem. Soc.* **2019**, *141* (15), 6191-6203.

(36) Musser, A. J.; Clark, J. Triplet-Pair States in Organic Semiconductors. *Annu. Rev. Phys. Chem.* **2019**, *70* (1), 323-351.

(37) Collins, M. I.; Campaioli, F.; Tayebjee, M. J. Y.; Cole, J. H.; McCamey, D. R. Quintet formation, exchange fluctuations, and the role of stochastic resonance in singlet fission. *Commun. Phys.* **2023**, *6* (1).

(38) Lukman, S.; Richter, J. M.; Yang, L.; Hu, P.; Wu, J.; Greenham, N. C.; Musser, A. J. Efficient Singlet Fission and Triplet-Pair Emission in a Family of Zethrene Diradicaloids. *J. Am. Chem. Soc.* **2017**, *139* (50), 18376-18385.